

High Temperature Erosion-Oxidation Behavior of Thermally Sprayed NiCr Based Alloy and Cermets Coatings

C. T. Kunioshi, O. V. Correa, L. V. Ramanathan

Corrosion Laboratory – Instituto de Pesquisas Energéticas e Nucleares, IPEN/SP

P. O. Box 11049, Pinheiros, CEP 05422-970, São Paulo, Brazil

Email: kunioshi@ipen.br, lalgudi@ipen.br

Abstract

The erosion-oxidation (E-O) behavior of high velocity oxy fuel (HVOF) sprayed Ni20Cr alloy as well as WC and Cr₃C₂ cermet coatings on a steel substrate were studied. The E-O tests were carried out in a rig with specimen assemblies that were rotated through a fluidized bed of erodent particles in the temperature range 500-850°C and with erodent impact velocities of 2.5-19.5 ms⁻¹. Alumina powder (~200µm) was used as the erodent. The E-O resistance of the coatings was determined as wastage, as a function of temperature. The three coatings did not exhibit any significant change in E-O at temperatures up to 500-600°C. At higher temperatures, wastage increased with temperature, reached a maximum at 700°C and then decreased with further increase in temperature. Different E-O regimes were identified. The specimen surfaces were examined in a scanning electron microscope and their roughness determined. E-O maps have been drawn that define conditions under which the coatings undergo low, moderate and severe wastage.

Keywords: Erosion, erosion-oxidation, erosion-oxidation maps, cermet coatings, composites, HVOF, surface roughness.

Introduction

The erosion behavior of metallic materials and ceramics at room temperature has been extensively studied¹⁻⁴. Nevertheless, a number of questions regarding correlations between erosion properties and physical parameters of the materials remain unanswered. A vast amount of information is available about the oxidation behavior of various metals and alloys at high temperatures⁵. However, only limited information is available about the conjoint effect of erosion and oxidation at high temperatures. The results of some of the erosion-oxidation (E-O) studies demonstrate that there is synergy between erosion and oxidation. This indicates that the degradation caused by E-O can be greater than the sum of degradation caused by erosion and oxidation processes operating separately⁶⁻¹⁰. It has also been mentioned that in some cases the corrosion products formed during oxidation inhibit erosion¹¹; i.e. the wastage rate under E-O conditions can be lower than that in the absence of oxidation. These contrary observations have generated, in recent years, much attention about E-O processes.

Hogmark et al. first described E-O interactions in terms of regimes in 1983¹². Kang et al. proposed the existence of four regimes as a function of increasing temperature, based on E-O studies of pure metals¹³. These regimes were termed: (a) erosion of metal, which predominated at low temperatures; (b) oxidation affected erosion, where the oxide and the metal eroded; (c) erosion-enhanced oxidation, during which more oxide formed as it was eroded and (d) oxide erosion, where only the oxide eroded. Modifications to these regimes and other interpretations about the existence of a variety of other sub E-O regimes have been proposed^{14,15}.

Procedures to combat E-O induced degradation are not readily available. At low temperatures, where oxidation is not a problem, hard coatings are often used. At higher temperatures, such coatings do not usually possess adequate corrosion resistance. The use of ceramic coatings

may address both, erosion and oxidation resistance. In recent years, the 'high velocity oxy fuel' (HVOF) process has sparked a considerable amount of commercial interest as it can produce smooth, low porosity, dense and adherent coatings. This process can be used to apply metal matrix composite coatings of Ni, Cr, Co or other alloys reinforced with carbides like WC or Cr_3C_2 on a variety of metallic substrates. These coatings impart increased wear resistance, especially at high temperatures, to the substrates. The HVOF process, as compared to plasma spraying, has the advantage of not altering the integrity of the carbide particles.

Nickel based alloys are often used for high temperature applications and contain sufficient chromium to form an external layer of chromium dioxide. Under cyclic oxidation conditions this oxide spalls due to the stresses in the oxide and difference in the coefficient of thermal expansion between the oxide and the underlying alloy. Nickel-chromium based alloy coatings reinforced with ceramic particles of WC and Cr_3C_2 have been used in many industrial applications to minimize degradation due to E-O^{16,17}. Many attempts have been made to explain the wear of these coatings and the interactions involved in the overall process, due to E-O¹⁸⁻²¹.

WC based composites, such as WC-Co, have been used in a variety of high temperature applications. WC-Ni composites have substituted WC-Co composites due to their higher oxidation resistance^{22,23}. Studies related to the oxidation behavior of WC, in powder form or in the as-sintered state have revealed that WC oxidized at temperatures beyond 500°C^{24,25}. In the initial stages of oxidation, parabolic kinetics was observed and this shifted to linear kinetics at temperatures beyond 700°C²². The oxide formed at 600°C was porous and at temperatures above 800°C mainly WO_3 , which fractured and spalled²⁶. Above 1.000°C, WC and its composites oxidized rapidly due to evaporation of WO_3 .

This paper presents the erosion-oxidation behavior of HVOF coatings of Ni20Cr alloy, and two cermets, WC 20Cr7Ni and Cr_3C_2 25(Ni20Cr). The E-O measurements were made in a

test rig in the temperature range 500-850°C, using alumina particles as the erodent at impact velocities in the range 2.5–19.5 ms⁻¹.

Materials and Methods

The HVOF process was used to apply coatings on AISI 310L sheet specimens 50 mm x 20mm. Powders with compositions corresponding to Ni20Cr, Cr₃C₂ 25(Ni20Cr) and WC 20Cr7Ni were used to produce the coatings. Specimens for the oxidation tests were cut to size from these coated sheets. Specimens for tests were cleaned, and degreased ultrasonically in acetone.

A schematic diagram of the E-O test rig was shown elsewhere²⁷. In this rig a specimen assembly was rotated through a fluidized bed of erodent particles. Alumina powder with particles in the size range 212-150 μm was used as the erodent. The fluidized bed of particles was obtained by pumping pre-heated air through a porous plate supporting a bed of erodent particles. Fluidization of the erodent particle was done within a furnace and a motor that rotated the specimen assembly controlled the erodent impact velocity on the test specimens.

The E-O test specimens were weighed and fixed with AISI 310 screws to the specimen holder in the E-O test rig. The specimens were positioned at the end of a crossed specimen holder. The E-O test conditions were: 500-850°C, two specimen rotation speeds with corresponding average erodent impact velocities of 3.5 and 14.8 ms⁻¹ at an impact angle of 90°. Tests were also carried out at 100°C to evaluate erosion behavior in the absence of oxidation. The particle impact velocity on the specimen varied depending on distance from the center of the axis. At distances of 5 mm, 25 mm and 45 mm from the near end of the specimen, the impact velocities at the two rotational speeds were 2.5, 3.5, 4.5 and 11.5, 14.8, 19.5 ms⁻¹ respectively. After the tests, the specimens were weighed, examined in a scanning electron microscope, the

surface reaction products analyzed by EDS and x-ray diffraction analysis and the surface roughness measured.

Results and Discussion

Erosion-oxidation behavior of coatings at erodent impact velocity of 3.5 ms⁻¹

The E-O behavior, expressed as wastage, of the three HVOF coatings as a function of temperature is shown in Figure 1. At particle impact velocity of 3.5 ms⁻¹ the three coatings did not exhibit any change in E-O behavior at temperatures up to 500-600°C, compared to at 100°C. However at higher temperatures, wastage increased with temperature, reaching a maximum at 700°C and then decreased with further increase in temperature up to 800°C. Above 800°C, wastage increased again. This E-O behavior is considered to be due to the formation of a spinel layer of NiCr₂O₄²⁸. This layer increases the ductility of the matrix (NiCr) and consequently, the E-O resistance. At particle impact velocity of 3.5 ms⁻¹, no significant differences in wastage between the Ni20Cr alloy coating and that of the cermet, Cr₃C₂ 25(Ni20Cr), were observed. This indicated that the mechanism of E-O of these two coatings was quite similar. The formation of the protective spinel type surface oxide prevented erosion of the coating. This E-O mechanism corresponds to a regime dominated as ‘substrate dominated’¹⁵. In this study assuming that the surface oxide cracked and its fragments got embedded in the substrate coating, giving rise to a composite of Ni20Cr, and mixed composites in the case of the other coatings, the results obtained do not differ from that in a purely erosive regime.

Increased wastage is observed between 600 and 700°C, due to erosion of the oxide which corresponds to the ‘oxide modified’ regime¹⁵ or ‘erosion affected by oxidation’ regime²⁹. At these temperatures, oxidation rate is higher than that at 600°C and consequently, oxide layer

thickness is also higher, but the internal stresses in the oxide being higher, aid the removal of oxide from the surface of the coating with erodent impact. Beyond 700°C, an increase in resistance to E-O is observed and the oxidation rate is higher than the rate of removal of oxide by erosion. Oxidation tests carried out with these coatings revealed that oxidation rates increased at temperatures beyond 700°C. This signifies that the surface oxide thickness increases. This behavior corresponds to ‘oxidation controlled erosion’²⁹ or ‘oxide dominated’ erosion¹⁵.

Insert Figure 1.

Above 800°C wastage rates increased. This phenomenon, still within the ‘oxidation controlled erosion’ regime was not mentioned in the early studies on erosion at high temperatures. One probable explanation for this behavior is that the oxide growth rate being higher at this temperature, reaches a critical stage where the internal stresses are high and sufficient to promote breakdown and spalling of the surface layer by the erodent. Besides this, formation of volatile products at temperatures beyond 850°C also sets in, contributing to mass loss of the coatings.

Comparison of the E-O behavior of the 3 coatings reveals that the Cr₃C₂ 25(Ni20Cr) coating has the highest resistance to E-O. Toma et al. reported the presence of NiCr₂O₄ oxide in as-deposited 75Cr₃C₂ 25NiCr HVOF coatings, decrease in grain size and the formation of a nanocrystalline structure²⁸. These factors are also considered to contribute to the E-O resistance of this coating.

The increased wastage of the WC coating at temperatures beyond 650°C is considered to be due to the formation of NiO and NiWO₄. However, the erosion process affects the oxidation of WC leading to formation of WO₃, which normally occurs at this temperature. This aspect is evident from the absence of spalling of the coatings, observed in the oxidation tests.

Between 700 and 800°C, increase in E-O resistance was observed, due to the higher oxidation rate, compared to removal of surface oxides by erosion. Above 800°C, a marked increase in wastage of this coating was observed. This is due to the 'oxide erosion' regime being operative. The oxidation rate increases with temperature and the oxide formed is brittle and non-protecting, independent of the nature of chromium-nickel oxide. Besides this, the oxidation rate of WC also increases forming WO_3 , which promotes cracking and subsequent spalling of the chromium oxide.

Erosion-oxidation behavior of coatings at erodent impact velocity of 14.8 ms^{-1}

Tests carried out at average erodent impact velocity of 14.8 ms^{-1} revealed a significant increase in E-O wastage of the coatings. At this higher impact velocity, wastage increased indicating changes in regime. In the case of the Ni20Cr coating a steady increase in wastage is seen and the 'oxidation controlled erosion' regime is not observed. This indicates that the oxide formed at temperatures up to 850°C, is not sufficient to decrease wastage under these conditions. The WC containing coating revealed better resistance to E-O at 750°C compared to at 700°C, indicating that the oxide layer formed at this temperature continuous to inhibit wastage. However, average wastage level, shown by mass loss, is high. In the case of the Cr_3C_2 25(Ni20Cr) coating, wastage at temperatures between 700 and 800°C is to the same extent, and the E-O resistance at 800°C is slightly higher, indicating that an increased rate of growth of an oxide layer impedes its removal by erodent impact.

Surface roughness and erosion-oxidation behavior

The thickness of the coatings after the E-O tests were measured to correlate wastage as a function of temperature and particle impact velocity and to confirm the results obtained from weight loss measurements. The thickness change data were not coherent, due mainly to the

non-uniform thickness of the HVOF coatings. Therefore surface roughness of the various test specimens was measured. Surface roughness profiles of the coatings E-O tested under the different conditions were determined. Figure 2 shows the mean surface roughness of the Ni20Cr, WC 20Cr7Ni and Cr₃C₂ 25(Ni20Cr) coatings as a function of temperature and erodent impact velocity. It can be observed that higher the surface roughness, lower the wastage. This confirms the observation made earlier that the surface oxide formed due to oxidation increases the E-O resistance, especially in the case of the WC 20Cr7Ni coating. Critical analysis of the surface roughness of the different coatings, as a function of temperature and erodent impact velocity, permitted the determination of wastage mechanisms at high temperatures. It also enabled the E-O behavior of the different coatings to be visualized, as a function of the different parameters.

Insert Figure 2.

Erosion-oxidation maps

An attempt to construct E-O maps for the three coatings was made using wastage and surface roughness measurement data. If Ra_i is the initial roughness of the coating, Ra the roughness of the coating after the test, values for low, moderate and severe wastage were defined as follows, for the test conditions, the coatings studied and based on criteria similar to that reported earlier³⁰: $Ra_i > Ra > 0.65 Ra_i$ as low wastage; $0.65 Ra_i > Ra > 0.3 Ra_i$ as moderate wastage; $0.3 Ra_i > Ra$ as severe wastage.

The limiting values of Ra (μm), that define low, moderate and severe wastage zones for the different coatings are shown in Table 1 and Figure 3. These values indicate basically that if wastage is sufficient to remove material from the surface (coating or the oxide formed on it), to decrease the coating's roughness, then its E-O resistance (Figure 3) can be considered to be

low wastage region at temperatures between 750 and 850°C at particle impact velocities of 4.5 ms^{-1} , a surprising behavior, considering the oxidation test results. This is due probably to steady removal of W oxide forming on the surface and consequent reduction if not elimination of WC that is inside the coating from oxidation and the formed oxide's expansion to expose even more of the coating surface. Hence, disintegration of this coating at this temperature is not observed.

Table 1. Limiting surface roughness values, Ra (μm), that define low, moderate and severe wastage zones for the different coatings, based on criteria adopted.

Coating	Wastage		
	low	moderate	severe
Ni20Cr	$5,0 > \text{Ra} > 2,2$	$2,2 > \text{Ra} > 1,5$	$1,5 > \text{Ra}$
WC 20Cr7Ni	$3,1 > \text{Ra} > 2,0$	$2,0 > \text{Ra} > 0,9$	$0,9 > \text{Ra}$
Cr₃C₂ 25(Ni20Cr)	$2,1 > \text{Ra} > 1,3$	$1,3 > \text{Ra} > 0,6$	$0,6 > \text{Ra}$

These wastage maps indicate qualitatively the conditions under which these coatings can be used with confidence. Evaluation of the E-O behavior of these coatings under other experimental conditions is in progress to extend the scope of the maps for use in materials selection.

Insert Figure 3.

Conclusions

1. Results of the erosion-oxidation tests carried out in an erosion-oxidation rig with alumina particles as the erodent revealed that the HVOF applied Cr₃C₂ 25(Ni20Cr)

coatings had the highest E-O resistance, compared to HVOF applied Ni20Cr and WC 20Cr7Ni coatings. This is due to the increased resistance of the oxide formed on the coatings surface.

2. The WC 20Cr7Ni coating revealed higher E-O resistance at temperatures between 750 and 850°C and at erodent impact velocity of up to 4.5 ms⁻¹ compared to its oxidation resistance. This indicated that the erosion process affects the E-O mechanism of this coating. Probable removal by the erodent of any W oxide that forms on the surface is considered to reduce or impede further rapid oxidation of WC inside the coating, and resultant expansion.
3. The E-O regimes for the three HVOF coatings were identified at erodent impact velocities of 2.5–4.5 ms⁻¹ and at temperatures between 100 and 850°C. At temperatures up to 600°C the wastage regime is ‘surface dominated’. Between 600 and 700°C the wastage corresponds to ‘oxide modified erosion-oxidation’ regime or ‘erosion affected by oxidation’. Beyond 700°C the E-O behavior corresponds to ‘oxidation controlled erosion’ or ‘oxide dominated’ behavior.
4. At higher erodent impact velocities, 11-19.5 ms⁻¹, the E-O wastage of the three coatings were significantly higher, indicating that the surface oxides formed at the high temperatures did not impede wastage.
5. Using surface roughness as the criterion to compare E-O behavior of the coatings, E-O maps were constructed for the different coatings. Regions corresponding to low, moderate and severe wastage have been defined and shown in the maps to aid in qualitative selection of conditions for safe use of the coatings.

References

1. Shewmon P, Sundararajan G. The erosion of metals. *Annual Review of Materials Science*. 1983; 13: 301-318.
2. Roy M., Tirupataiah Y., Sundararajan G. Effect of particle shape on the erosion of Cu and its alloys. *Materials Science and Engineering A*. 1993; 165(1): 51-63.
3. Bitter JGA. A study of erosion phenomena Part II. *Wear*. 1963; 6(3): 169-190.
4. Hutchings IM, Winter RE. Particle erosion of ductile metals – mechanism of material removal. *Wear*. 1974; 27(1): 121-128.
5. Wood, G.C., *Oxidation of Metals*, 2, 11, 1970.
6. Ives LK. Erosion of 310 stainless steel at 975 degrees C in combustion gas atmospheres. *Journal of Engineering Materials and Technology - Transactions of the ASME 99 (2)*. 1977; 126-132.
7. Bhattacharya S, Hales C, Hill V. Erosion-Corrosion of Materials in Coal Gasifier Environments. In: Natesan K, editor. *Proceedings of the Fall Meeting of The Metallurgical Society of AIME*; 1978 Oct 17-18; St. Louis, USA. New York: The Metallurgical Society of AIME; 1980. p. 244-267.
8. Wright IG, Nagarajan V, Herchenroeder RB. Some Factors Affecting Solid Particle Erosion/Corrosion of Metals and Alloys. In: Natesan K, editor. *Proceedings of the Fall Meeting of The Metallurgical Society of AIME*; 1978 Oct 17-18; St. Louis, USA. New York: The Metallurgical Society of AIME; 1980. p. 268-312.
9. Zambelli G, Levy AV. Particulate erosion of NiO scales. *Wear*. 1981; 68(3): 305-331.
10. Tabakoff W. Experimental-study on the effects of specimen sizes on erosion. *Wear*. 1983; 86(1): 65-72.

11. Stack MM, Lekatos S, Stott FH. Erosion-corrosion regimes: number, nomenclature and justification?. *Tribology International*. 1995; 28(7): 445-451.
12. Hogmark S, Hammarsten A, Söderberg S. On the Combined Effects of Corrosion and Erosion. In: Cavendish Laboratory Publisher. *Proceedings of Sixth International Conference Erosion by Solid and Liquid Impact*; 1983 Sept. 5-8; Cambridge, UK. Cambridge: Cavendish Laboratory - University of Cambridge; 1983. Paper 37, 8 pp.
13. Kang CT, Pettit FS, Birks N. Mechanisms in the simultaneous erosion-oxidation attack of nickel and cobalt at high temperature. *Metallurgical Transactions A – Physical Metallurgy and Materials Science*. 1987; 18(10): 1785-1803.
14. Rishel DM, Pettit FS, Birks N., Some principal mechanisms in the simultaneous erosion and corrosion attack of metals at high temperatures. *Materials Science and Engineering A – Structural Materials Properties, Microstructure and Processing*. 1991; 143 (1-2): 197-211.
15. Stephenson DJ, Nicholls JR. Modeling Erosive Wear. *Corrosion Science*. 1993; 35(5-8): 1015-1026.
16. Walsh PN, Tabakoff W, Power 10, 1, 1990.
17. Walsh PN. Erosion resistance of coatings at steam turbine temperatures. In: ASME Publisher. *Proceedings of International Joint Power Generation Conference*; 1992 Oct. 18-22; Atlanta, USA. New York: The Metallurgical Society of AIME; 1992. p. 123-128.
18. Levy A.V. The erosion-corrosion behavior of protective coatings. *Surface and Coatings Technology*. 1988; 36(1-2): 387-406.
19. Tu J.P., Liu M.S., Mao Z.Y. Erosion resistance of Ni-WC self-fluxing alloy coating at high temperature. *Wear*. 1997; 209(1): 43-48.
20. Wang B.Q., Geng G.Q., Levy A.V. Erosion-corrosion of thermal spray coatings. *Surface and Coatings Technology*. 1990; 43-44(1): 859-874.

21. Stack M.M., Pena D. Solid particle erosion of Ni-Cr/WC metal matrix composites at elevated temperatures: construction of erosion mechanism and process control maps *Wear*. 1997; 203-204: 489-497.
22. Ekemar S., Lindholm I., Hartzel T. *International Journal of Refractory Metals and Hard Materials*. 1982; 1: 37-.
23. Suzuki H., Hayashi K., Terada O. *J. Jap. Inst. Metals*, 41, 559, 1977
24. Webb W.W., Norton J.T., Wagner C. *Journal of Electrochemical Society*. 1956; 103: 112.
25. Newkirk, A.E. The oxidation of tungsten carbide. *Journal of American Chemical Society*. 1955; 77(17): 4521-4522.
26. Voitovich V.B., Sverdel V.V., Voitovich R.F., Golovko E.I. Oxidation of WC-Co, WC-Ni and WC-Co-Ni hard metals in the temperature range 500–800°C. *International Journal of Refractory Metals and Hard Materials*. 1996; 14(4): 289-295.
27. Kuniishi CT, Correa OV, Ramanathan LV. Influence of processing parameters on the microstructure and oxidation behavior of hot pressed Ni-20Cr+WC metal matrix composites. *Materials Science Forum*. 2005; 403(4): 195-200.
28. Toma D, Brandl W, Marginean G. Wear and corrosion behaviour of thermally sprayed cermet coatings. *Surface and Coatings Technology*. 2001; 138(2-3): 149-158.
29. Sundararajan G. The solid particle erosion of metallic materials at elevated temperatures. *Proceedings of 4th Berkeley Conference on Corrosion-Erosion-Wear of Materials at Elevated Temperatures*; 1990; Berkeley, USA. Houston: NACE; A.V. Levi (ed.), 1991, paper 11, p. 1-33.
30. Stack M.M., Stott F.H., Wood G.C. Review of mechanisms of erosion-corrosion of alloys at elevated temperatures. *Wear*. 1993; 162-164: 706-712.

Figure Captions

Figure 1. E-O behavior, expressed as wastage, of the three types of HVOF coatings on AISI 310 as a function of temperature. The full and dotted lines correspond to average impact velocities of 3.5 and 14.8 ms^{-1} respectively.

Figure 2. Mean surface roughness, R_a , as a function of temperature of Ni20Cr (a), WC 20Cr7Ni (b) and Cr_3C_2 25(Ni20Cr) (c) specimens E-O tested with different impact erodent velocities.

Figure 3. E-O maps of HVOF coatings of (a) Ni20Cr, (b) WC 20Cr7Ni and (c) Cr_3C_2 25(Ni20Cr). The maps show the wastage zones based on mean surface roughness criterion, as a function of temperature and erodent impact velocities.

Figures

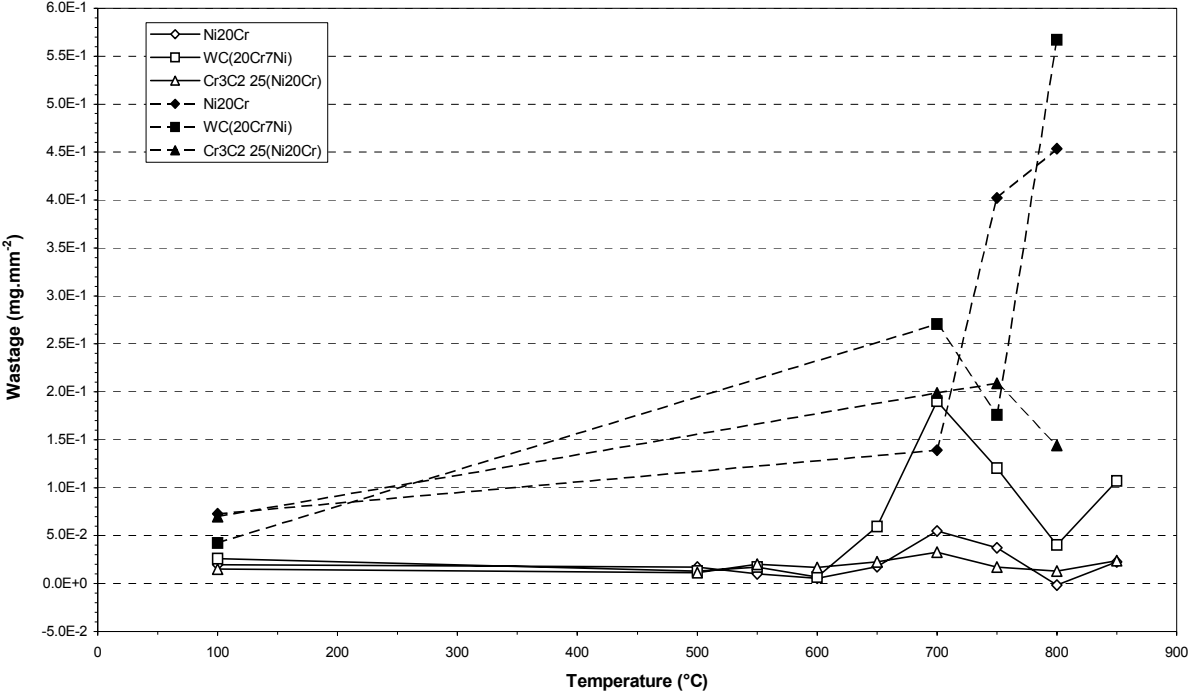
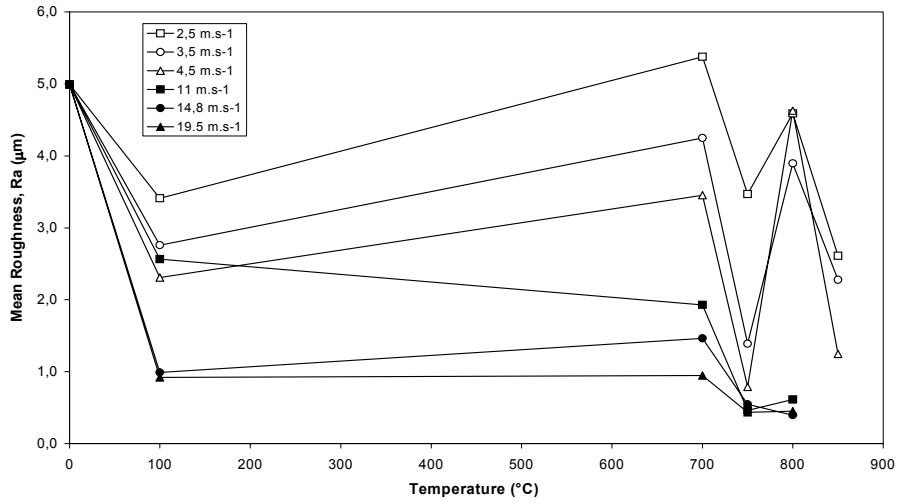
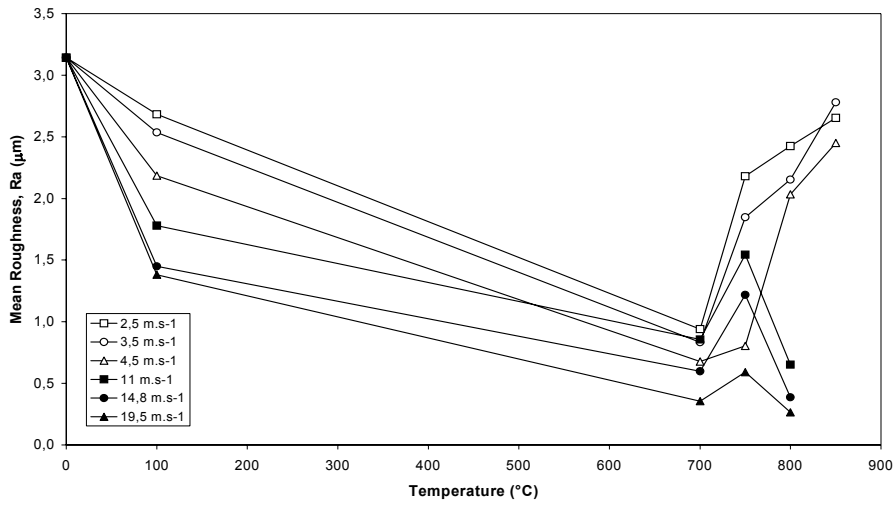


Figure 1.

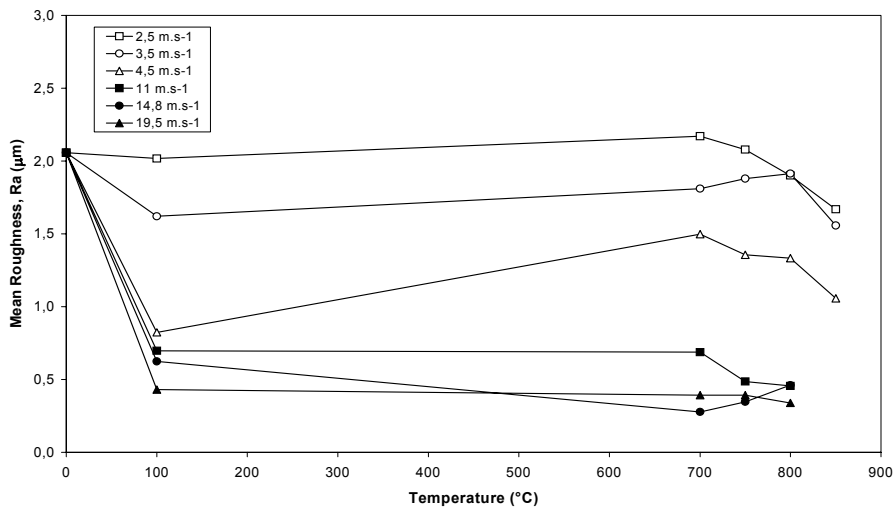
C. T. Kunioshi, O. V. Correa, L. V. Ramanathan



(a)



(b)



(c)

Figure 2.

C. T. Kunioshi, O. V. Correa, L. V. Ramanathan

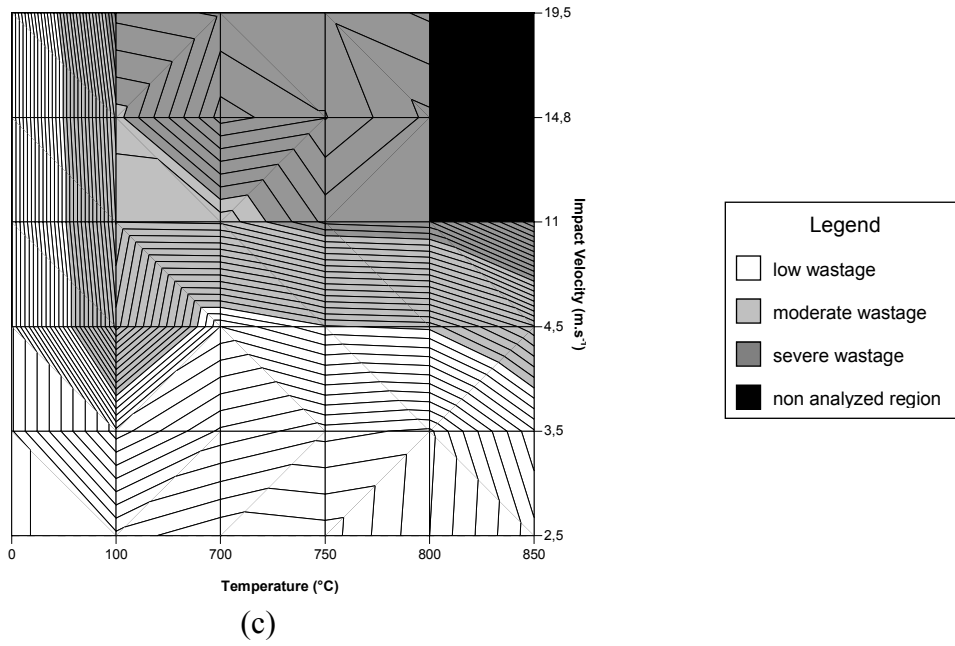
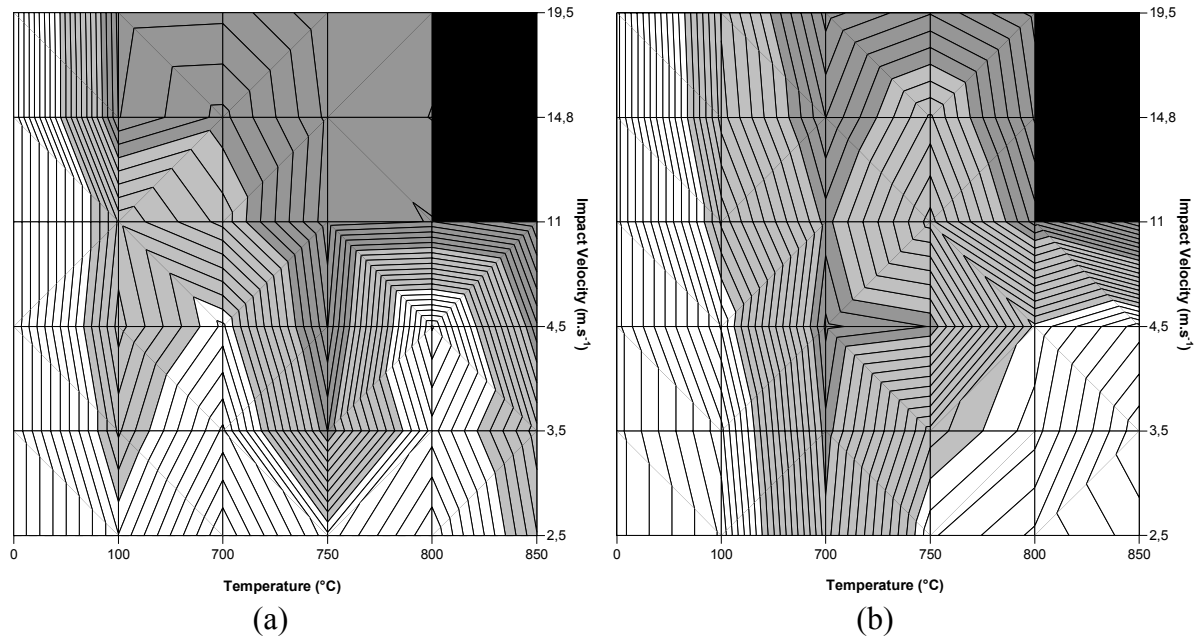


Figure 3.

C. T. Kunioshi, O. V. Correa, L. V. Ramanathan